Electronic Research Archive

https://www.aimspress.com/journal/era

ERA, 34(3): 2066–2086.
DOI: 10.3934/era.2026092
Received: 29 December 2025
Revised: 23 February 2026
Accepted: 27 February 2026
Published: 06 March 2026

Research article

L1/finite element methods for time-fractional Keller-Segel equations with weak singularity solution

Jia Xie[1] **and Qingfeng Li**[2,*]

[1] School of Educational Science, Gannan Normal University, Ganzhou 341000, China

[2] School of Mathematics and Computer Sciences, Gannan Normal University, Ganzhou 341000, China

* **Correspondence:** Email: lqfmath@163.com.

Abstract: In this paper, we consider the L1/ finite element methods for solving time-fractional Keller-Segel equations with a singular solution. For time direction, the L1 scheme under the nonuniform mesh is considered to approximate the Caputo derivative to handle the singularity of the solution. To further reduce computational storage requirements, we consider a fast L1 scheme based on the sum-of-exponentials skill for calculating fractional derivatives. Then, we derive a fully implicit discrete scheme by combining the finite element method in the spatial direction. Subsequently, unconditional stability and α-robust error estimates of the fully discrete scheme are derived. Finally, numerical examples are presented to verify our theory.

Keywords: time-fractional Keller-Segel equations; L1 scheme; finite element method; unconditional stability; α-robust error estimates

1. Introduction

Chemotaxis, the directed movement of biological entities in response to chemical concentration gradients, is a fundamental process underlying numerous biological phenomena. In the 1970s, Keller and Segel [1, 2] first proposed Keller-Segel (KS) equations, which have since become the classical mathematical model for describing chemotaxis. Generally, the simplest form of this model can be written as

$$\begin{cases} \partial_t u - \Delta u + \nabla \cdot (u \nabla v) = 0, & \mathbf{x} \in \Omega,\ 0 < t < T, \\ \partial_t v - \Delta v + v = u, & \mathbf{x} \in \Omega,\ 0 < t < T. \end{cases} \tag{1.1}$$

Here, Ω is a bounded domain in $\mathbb{R}^d (d \geq 1)$ with a smooth boundary $\partial\Omega$, $u(\mathbf{x}, t)$, which represents the density of bacteria, and $v(\mathbf{x}, t)$ stands for the concentration of oxygen. This model exhibits rich

mathematical structures, and the properties of its solutions, such as global boundedness and blow-up behavior, are closely related to the spatial dimension. There are already very rich theoretical results; see [3]. At the same time, researches on the numerical schemes of this model have also conducted extensive research via the finite difference method [4, 5], finite volume method [6], finite element method [7], and spectral method [8, 9].

Biological systems often exhibit memory-dependent dynamics. An example is delayed responses to chemical signals or non-Markovian migration patterns wherein the evolution of the system depends not only on the current state but on its entire history [10, 11]. These characteristics cannot be adequately modeled by integer-order derivatives, motivating the extension of the classical KS framework to time-fractional Keller-Segel (TFKS) equations. Because the Caputo derivative has a nonlocal time dependence via a convolution kernel $t^{-\alpha}$, it enables the modeling of anomalous diffusion and long-range temporal correlations. Here, we replace the first-order time derivative in the density equation and concentration equation with the Caputo fractional derivative, yielding

$$\begin{cases} \partial_t^\alpha u - \Delta u + \nabla \cdot (u \nabla v) = 0, & \mathbf{x} \in \Omega,\ 0 < t < T, \\ \partial_t^\alpha v - \Delta v + v = u, & \mathbf{x} \in \Omega,\ 0 < t < T. \end{cases} \tag{1.2}$$

For the subsequent numerical simulation, we assume that the initial condition and the boundary condition are

$$\begin{cases} u(x,0) = u_0(x), \quad v(x,0) = v_0(x), & \mathbf{x} \in \Omega, \\ u(x,t) = v(x,t) = 0, & \mathbf{x} \in \partial\Omega, 0 < t < T. \end{cases} \tag{1.3}$$

Here, u_0, v_0 are known functions, and $\partial_t^\alpha u$ is defined as

$$\partial_t^\alpha u = \int_0^t \omega_{1-\alpha}(t-\xi) u'(\xi) d\xi, \quad 0 < \alpha < 1 \tag{1.4}$$

with the kernel $\omega_\alpha(t) = t^{\alpha-1}/\Gamma(\alpha)$. The $\partial_t^\alpha v$ is defined analogously. This generalization enhances the model biological realism: the fractional order α quantifies the "memory strength" of the system, with $\alpha \to 1$ recovering the classical KS equation.

The theoretical analysis of TFKS equations presents unique challenges compared to the KS equations. Key problems include the well-posedness and nonnegativity of solutions, their long-time behavior, and the persistence of critical phenomena such as finite time blow up. In [12, 13], the existence and uniqueness of weak solutions were established under suitable regularity conditions. Bezerra et. al. [14] derived the long-time behavior of solutions and studied the well-posedness and the asymptotic stability of solutions in Marcinkiewicz spaces. In [15], the well-posedness and blow-up behavior of solutions was studied. At the same time, several techniques have been used to derive analytical solutions, such as Adomian decomposition methods and homotopy function methods [16]. However, the aforementioned methods require the imposition of strict conditions to get analytical solutions, and the analytical solutions obtained are limited. It is therefore of great significance to consider the numerical solution of TFKS equations.

As far as we know, the numerical schemes of TFKS equations were only mentioned in [17]. The authors developed a fractional class of explicit Adams–Bashforth and implicit Adams–Moulton schemes on the uniform meshes for solving nonlinear fractional-order differential systems with Caputo derivatives and further applied these schemes to solve fractional KS equations. Meanwhile,

first- and second-order accuracy are derived under the assumption of a sufficiently smooth solution. Nevertheless, the ubiquitous feature of solution is weakly singular near the initial time $t = 0$ [18–20]. This makes the existing numerical schemes with uniform time meshes often less accurate, such as the convergence order derived by the uniform L1 scheme is only α in [20]. The graded time meshes provide an efficient way of computing a reliable numerical solution near time $t = 0$. It be seen that the L1 scheme based on the graded meshes can achieve the optimal convergence order of $(2 - \alpha)$ from [21–23], and this technique can be extended to higher-order numerical schemes, such as the L2 scheme [24] and L2-1_σ scheme [25]. Moreover, the nonlocality of the fractional derivatives shall cause all the aforementioned schemes to require $O(N^2)$ computational cost for N time steps, which are too expensive. Then, the fast algorithms to reduce computational cost have been developed. For instance, Jiang et al. [26] presented the sum-of-exponentials (SOE) method to speed up the evaluation of a weakly singular Caputo derivative kernel, which greatly reduces the computational cost. Similarly, the fast L1, L2, and L2-1_σ schemes are presented on both uniform and nonuniform meshes in [27, 28].

The main goal of this paper is to develop a numerical scheme to efficiently solve the problems (1.2) and (1.3). Obviously, the design of an efficient technique to numerically solve this problem is not an easy task. The main difficulties are given by the singularity and nonlocality of fractional derivatives and the strong nonlinearity of the problem itself. To overcome these difficulties, we first apply the L1 scheme and the fast L1 scheme on the graded mesh to approximate the time-fractional derivative and use the finite element method to discrete the spatial direction, thus deriving a fully implicit scheme. This scheme is stable and has higher accuracy compared to explicit schemes. We then provide a rigorous proof process. Furthermore, we shall utilize the theoretical framework presented in [29, 30] to investigate an α-robust error estimate for the fully discrete scheme. The main contributions of our work are as follows: 1) We firstly consider the numerical method for solving time-fractional KS models with singular cases. Compared to the smooth case in reference [17], our numerical method is more in line with the characteristics of fractional order models. 2) We prove the stability of the numerical scheme both the $L^2(\Omega)$ and $H^1(\Omega)$ norms under some constraints on the time-step ratio and obtain an α-robust error estimate by the fractional Grönwall inequality. We note that this theoretical analysis framework is also applicable to the more complex time-fractional coupled diffusion systems.

The outline of this paper is as follows. In Section 2, we recall the finite element space and the L1 scheme, and the fully discrete scheme is introduced. In Section 3, the unconditional stability of the fully discrete scheme in both $L^2(\Omega)$ and $H^1(\Omega)$ norms is proved. In Section 4, we derive an α-robust error estimate in both $L^2(\Omega)$ and $H^1(\Omega)$ norms. In Section 5, we present a fast L1/finite element scheme for solving TFKS equations, and provide a brief description. In Section 6, we present an example with numerical results to verify our theorems. Some conclusions are provided in Section 7.

2. A fully discrete L1/finite element scheme for the time fractional Keller-Segel equations

Let $L^p(\Omega)$ be the Lebesgue space with norm $\|\cdot\|_{0,p}$ for $0 \le p \le \infty$. We denote as $W^{k,p}(\Omega)$ the Sobolev space with norm $\|\cdot\|_{k,p}$ given by

$$\|u\|_{k,p} = \begin{cases} \Big(\sum\limits_{|\alpha|\le k} \big(\|D^\alpha u\|_{0,p}^p\big)^{1/p}, & 1 \le p < \infty, \\ \max\limits_{|\alpha|\le k} \|D^\alpha u\|_{0,\infty}, & p = \infty. \end{cases} \tag{2.1}$$

When $k = 0$, we have $W^{0,p}(\Omega) = L^p(\Omega)$, and we have $W^{k,2}(\Omega) = H^k(\Omega)$ is Hilbert space for $p = 2$. Specially, we define as $H_0^k(\Omega) = \{v \in H^k(\Omega) : v|_{\partial\Omega} = 0\}$. For the sake of simplicity, we write $\|v\|_{L^2(\Omega)} = \|v\|$ and $\|v\|_{H^k(\Omega)} = \|v\|_k$. and use the letter C to denote a positive constant independent of the mesh size and the time step size.

A weak formulation of problems (1.2) and (1.3) reads: Find $(u, v) \in H_0^1(\Omega) \times H_0^1(\Omega)$ such that

$$\begin{cases} (\partial_t^\alpha u, w) + (\nabla u, \nabla w) - (u\nabla v, \nabla w) = 0, & w \in H_0^1(\Omega), \\ (\partial_t^\alpha v, w) + (\nabla v, \nabla w) + (v, w) = (u, w), & w \in H_0^1(\Omega), \\ u(x, 0) = u_0,\ v(x, 0) = v_0. \end{cases} \tag{2.2}$$

According to the results of [13], it is known that there exists a unique weak solution $u, v \in L^\infty([0, T]; L^2(\Omega)) \cap L^2([0, T]; H_0^1(\Omega))$ for the above weak formulation.

Now, we recall the L1 scheme on the graded meshes for approximating the Caputo fractional derivative. Let $0 = t_0 < t_1 < \cdots < t_N = T$ be a nonuniform partition of the time interval $[0, T]$ with step size $\tau_k = t_k - t_{k-1} (1 \le k \le N)$ and the time points

$$t_k = T(k/N)^r, \quad k = 1, 2, \cdots, N, \tag{2.3}$$

where $r \ge 1$ is the grading parameter. Note that the time mesh is uniform when $r = 1$. Assume that there exists a constant ρ such that $\tau_k/\tau_{k+1} < \rho$ for $1 \le k \le N$. We set $\varphi^n = \varphi(t_n)$ and $\nabla_\tau \varphi^k = \varphi^k - \varphi^{k-1}$ for $0 < k < N$. Thus, for the Caputo fractional derivative $\partial_t^\alpha \varphi(t)$ at $t = t_n$, the nonuniform L1 scheme is given by

$$\begin{aligned} \partial_t^\alpha \varphi^n &= \sum_{k=0}^{n-1} \int_{t_k}^{t_{k+1}} \omega_{1-\alpha}(t_k - \xi)\varphi'(\xi) d\xi \\ &\approx \frac{1}{\Gamma(1-\alpha)} \sum_{k=0}^{n-1} \frac{\varphi^{k+1} - \varphi^k}{\tau_{k+1}} \int_{t_k}^{t_{k+1}} \frac{ds}{(t_n - s)^\alpha} \\ &= \sum_{k=1}^{n} a_{n,k} \nabla_\tau \varphi^k =: \bar{\partial}_\tau^\alpha \varphi^n, \end{aligned} \tag{2.4}$$

where the corresponding coefficients is

$$a_{n,k} = \frac{1}{\tau_k \Gamma(1-\alpha)} \int_{t_{k-1}}^{t_k} (t_n - s)^{-\alpha} ds = \frac{(t_n - t_{k-1})^{1-\alpha} - (t_n - t_k)^{1-\alpha}}{\tau_k \Gamma(2-\alpha)}, \ 1 \le k \le n. \tag{2.5}$$

Especially, $a_{n,n} = \tau_n^{-\alpha}/\Gamma(2-\alpha)$, and by the mean value theorem, it is shown that

$$0 < a_{n,k} < a_{n,k+1}, \quad k = 1, 2, \cdots, n-1. \tag{2.6}$$

Assume that $|\varphi^{(l)}(t)| \le C(1 + t^{\alpha-l})$ for $l = 0, 1, 2$. We shall derive the following truncation error [19]:

$$\left|\partial_t^\alpha \varphi(t_n) - \bar{\partial}_\tau^\alpha \varphi^n\right| \le C n^{-\min\{2-\alpha, r\alpha\}}, \quad n = 1, 2, \cdots, N. \tag{2.7}$$

Moreover, it is shown in [31] that the inner product of operator $\bar{\partial}_\tau^\alpha$ satisfies the the following inequality

$$(\bar{\partial}_\tau^\alpha \varphi(t_n), \varphi(t_n)) \ge \frac{1}{2} \bar{\partial}_\tau^\alpha \|\varphi(t_n)\|^2. \tag{2.8}$$

Inspired by [21], we define the discrete convolution kernels as

$$P_{n,0} = \frac{1}{a_{n,n}}, \quad P_{n,n-j} = \frac{1}{a_{j,j}} \sum_{k=j+1}^{n} \left(a_{k,k-j-1} - a_{k,k-j}\right) P_{n,n-k}, \ 1 \le j \le n-1.$$

It is known that the above-mentioned convolution kernel satisfies the following properties [28, 29]:

$$\sum_{j=1}^{n} P_{n,n-j} j^{r(l_N-\alpha)} \le \frac{11\Gamma(1+l_N-\alpha)}{4\Gamma(1+l_N)} T^{\alpha} \left(\frac{t_n}{T}\right)^{l_N} N^{r(l_N-\alpha)}, \quad \forall\ l_N \in (0,1), \tag{2.9}$$

$$\sum_{j=1}^{n} P_{n,n-j} \left|\partial_t^{\alpha} u(t_n) - \bar{\partial}_{\tau}^{\alpha} u(t_n)\right| \le C_T N^{-min\{2-\alpha, r\alpha\}}, \tag{2.10}$$

$$\sum_{j=1}^{n} P_{n,n-j} \le \frac{11}{4\Gamma(1+\alpha)} t_n^{\alpha}. \tag{2.11}$$

The last property can be derived by setting $l_N = \alpha$ in Eq (2.9).

To derive the robust theoretical results, we shall introduce the improved discrete fractional Grönwall inequality [28, 32, 33].

Lemma 2.1. *For any nonnegative sequences* $\{\xi^n\}_{n=1}^N$,$\{\eta^n\}_{n=1}^N$,*and* $\{\lambda_k\}_{n=1}^{N-1}$, *suppose there exists a constant* Λ *such that* $\sum\limits_{k=0}^{N-1} \lambda_k \le \Lambda$ *for* $N \ge 1$. *Let the grid function* $\{\varphi^k\}_{k=0}^N$ *satisfy*

$$\bar{\partial}_{\tau}^{\alpha}(\varphi^k)^2 \le \sum_{k=1}^{n} \lambda_k (\varphi^k)^2 + \xi^n \varphi^n + (\eta^n)^2. \tag{2.12}$$

If the maximum step size $\tau^* \le (2\Gamma(2-\alpha)\Lambda)^{-1/\alpha}$ *holds, it follows that, for* $1 \le n \le N$,

$$\varphi_n \le 2E_{\alpha}(2\Lambda t_n^{\alpha}) \left(\varphi_0 + \max_{1\le k\le n} \sum_{j=1}^{k} P_{k,k-j}(\xi^j + \eta^j) + \max_{1\le j\le n}\{\eta^j\}\right), \tag{2.13}$$

where

$$E_{\alpha,\beta}(z) = \sum_{k=0}^{\infty} \frac{z^k}{\Gamma(\beta + k\alpha)}$$

is the Mittag-Leffler function, and $E_{\alpha}(z) = E_{\alpha,1}(z)$.

Based on the L1 scheme (2.4), we introduce the following semidiscrete scheme at time t_n: Find $(U^n, V^n) \in (H_0^1(\Omega) \times H_0^1(\Omega))$ for $n = 1, 2, \cdots, N$, such that

$$\begin{cases} (\bar{\partial}_{\tau}^{\alpha} U^n, w) + (\nabla U^n, \nabla w) - (U^n \nabla V^n, \nabla w) = 0, & w \in H_0^1(\Omega). \\ (\bar{\partial}_{\tau}^{\alpha} V^n, w_h) + (\nabla V^n, \nabla w) + (V^n, w) = (U^n, w), & w \in H_0^1(\Omega). \\ U^0 = u_0, \ V^0 = v_0. \end{cases} \tag{2.14}$$

Utilizing the Duhamel's principle, we derive the representation to the solution of the problem (1.2):

$$u(t) = E_{\alpha}(t^{\alpha}\Delta)u_0 - \int_0^t (t-s)^{\alpha-1} E_{\alpha,\alpha}((t-s)^{\alpha}\Delta)\nabla \cdot (u\nabla v)(s) ds, \tag{2.15}$$

$$v(t) = E_\alpha(t^\alpha(\Delta - 1))v_0 + \int_0^t (t-s)^{\alpha-1} E_{\alpha,\alpha}((t-s)^\alpha(\Delta-1))u(s)ds, \tag{2.16}$$

Furthermore, we calculate the gradient of (2.16) to yield

$$\nabla v(t) = E_\alpha(t^\alpha(\Delta - 1))\nabla v_0 + \int_0^t (t-s)^{\alpha-1} \nabla E_{\alpha,\alpha}((t-s)^\alpha(\Delta-1))u(s)ds. \tag{2.17}$$

Usually, we refer to the above solutions as "mild solutions". By the mild solution (2.15)–(2.17), we can obtain a prior bounds of the solution in the problem (1.2).

Lemma 2.2. *[14] Assume that $u_0 \in L^1(\Omega), v_0, \nabla v_0 \in L^1(\Omega) \cap L^\infty(\Omega)$ are necessarily small. Then, there exists a unique global solution $(u, v) \in \mathbb{R}^2 \times (0, +\infty)$ to the problem* (1.2)*, and it that*

$$\sup_{t>0}(\|u(t)\|_{L^\infty(\Omega)} + \|v(t)\|_{L^\infty(\Omega)}) < \infty, \quad \sup_{t>0} \|\nabla v(t)\|_{L^\infty(\Omega)} < \infty,$$

and it has the following time decay behavior:

$$\sup_{t>0}(\|u(t)\|_{L^\infty(\Omega)} + \|v(t)\|_{L^\infty(\Omega)}) < C(1+t)^{-\alpha/\mu},$$
$$\sup_{t>0} \|\nabla v(t)\|_{L^\infty(\Omega)} \le C(1+t)^{-\alpha/\mu},$$

where $1 < \mu < 2$.

Inspired by Lemma 2.2, we suppose that ∇v is bounded, that is, there exists a positive constant M, such that

$$\|\nabla v\|_{L^\infty(\Omega)} \le M. \tag{2.18}$$

We now split $\|\nabla V^n\|_{L^\infty(\Omega)}$ into

$$\|\nabla V^n\|_{L^\infty(\Omega)} \le \|\nabla v^n\|_{L^\infty(\Omega)} + \|\nabla(v^n - V^n)\|_{L^\infty(\Omega)}.$$

Then, we will derive the boundedness of ∇V^n for $n = 0, 1, 2, \dots N$, satisfying

$$\|\nabla V^n\|_{L^\infty(\Omega)} \le M, \tag{2.19}$$

whenever $\tau \le \tau_a = (C_\Omega C_T)^{-1/\min(r\alpha, 2-\alpha)}$, and here $M = \max\limits_{0\le n\le N} \|\nabla v^n\|_{L^\infty(\Omega)} + 1$, and C_Ω is a constant related only to the domain Ω, and C_T is a constant related only to the final time T.

Let $\mathcal{T}_h = \bigcup K$ be a uniform mesh partition of Ω with mesh size h. We denote by $S_h \subset H_0^1(\Omega)$ the standard finite element space satisfying the homogeneous Dirichlet condition. Let $R_h : H_0^1(\Omega) \to S_h$ be a Ritz projection operator satisfying

$$(\nabla(u - R_h u), w_h) = 0, \quad w \in S_h. \tag{2.20}$$

Then, the following error estimate holds [34]:

$$\|u - R_h u\| + h\|u - R_h u\|_1 \le Ch^{k+1}\|u\|_{k+1} \tag{2.21}$$

for any $u \in H^{k+1}(\Omega) \cap H_0^1(\Omega)$.

Combining the L1 scheme (2.4) and finite element method, we construct a fully implicit discrete scheme: Find $(U_h^n, V_h^n) \in S_h \times S_h$, for $n = 1, 2, \ldots, N$, such that

$$\begin{cases} (\bar{\partial}_\tau^\alpha U_h^n, w_h) + (\nabla U_h^n, \nabla w_h) - (U_h^n \nabla V_h^n, \nabla w_h) = 0, \quad w_h \in S_h, \\ (\bar{\partial}_\tau^\alpha V_h^n, w_h) + (\nabla V_h^n, \nabla w_h) + (V_h^n, w_h) = (U_h^n, w_h), \quad w_h \in S_h, \\ U_h^0 = R_h u_0, \ V_h^0 = R_h v_0. \end{cases} \tag{2.22}$$

Similar to (2.19), and utilizing the inverse inequality, we have

$$\begin{aligned} \|\nabla V_h^n\|_{L^\infty}(\Omega) &\le \|\nabla R_h V^n\|_{L^\infty}(\Omega) + \|\nabla(R_h V^n - V_h^n)\|_{L^\infty}(\Omega) \\ &\le \|\nabla R_h V^n\|_{L^\infty(\Omega)} + Ch^{-1}\|\nabla(R_h V^n - V_h^n)\| \\ &\le \|\nabla R_h V^n\|_{L^\infty(\Omega)} + Ch^{-1}h^k\|v\|_k. \end{aligned}$$

Thus, when v is sufficiently smooth, we shall obtain that the solutions of the problem (2.22) is bounded, i.e., for $n = 0, 1, 2, \cdots, N$, there exists a positive constant M, such that

$$\|\nabla V_h^n\|_{L^\infty(\Omega)} \le M. \tag{2.23}$$

3. Stability analysis of the L1/finite element scheme

In this section, we shall discuss the stability of the full discrete scheme (2.22) in both $L^2(\Omega)$ and $H^1(\Omega)$ norms, and the results are as follows.

Theorem 3.1. *For $n = 0, 1, 2, \ldots, N$, the fully discrete scheme* (2.22) *satisfies the following stability results:*

$$\|U_h^n\| + \|V_h^n\| \le C\left(\|U_h^0\| + \|V_h^0\|\right). \tag{3.1}$$

$$\|U_h^n\|_1 + \|V_h^n\|_1 \le C\left(\|U_h^0\|_1 + \|V_h^0\|_1\right), \tag{3.2}$$

where C is an α-robust constant.

Proof. Taking $w_h = U_h^n$ in the first equation of the fully discrete scheme (2.22), using the Cauchy-Schwartz inequality and Young's inequality yields

$$\begin{aligned} (\bar{\partial}_\tau^\alpha U_h^n, U_h^n) + (\nabla U_h^n, \nabla U_h^n) &= (U_h^n \nabla V_h^n, \nabla U_h^n) \\ &\le \|\nabla V_h^n\|_{L^\infty(\Omega)} \|U_h^n\| \|\nabla U_h^n\| \\ &\le \varepsilon \|\nabla U_h^n\|^2 + \frac{M}{\varepsilon}\|U_h^n\|^2, \quad \varepsilon \in (0, 1). \end{aligned}$$

By the discrete fractional Grönwall inequality (2.12) and (2.8), we have

$$\|U_h^n\| \le 2E_\alpha\left(\frac{2M}{\varepsilon} t_n^\alpha\right)\|U_h^0\|. \tag{3.3}$$

Setting $w_h = V_h^n$ in the second equation of the fully discrete scheme (2.22), we have

$$(\bar{\partial}_\tau^\alpha V_h^n, V_h^n) + (\nabla V_h^n, \nabla V_h^n) + (V_h^n, V_h^n) = (U_h^n, V_h^n). \tag{3.4}$$

Then, using Young's inequality and (2.8), we get

$$\bar{\partial}_\tau^\alpha \|V_h^n\|^2 \le 2\|U_h^n\|\|V_h^n\| \le \|U_h^n\|^2 + \|V_h^n\|^2. \tag{3.5}$$

Therefore, by the discrete fractional Grönwall inequality for (2.12) and (3.3), we get

$$\begin{aligned} \|V_h^n\| &\le 2E_\alpha(2t_n^\alpha)\left(\|V_h^0\| + \max_{1\le j\le n}\|U_h^j\|\right) \\ &\le 2E_\alpha(2t_n^\alpha)\left(\|V_h^0\| + 2E_\alpha\left(\frac{2M}{\varepsilon}t_n^\alpha\right)\|U_h^0\|\right). \end{aligned} \tag{3.6}$$

The proof of Eq (3.1) has been completed.

Let $w_h = \bar{\partial}_\tau^\alpha U_h^n$ in the first equation in the fully discrete scheme (2.22). We have

$$\begin{aligned} (\bar{\partial}_\tau^\alpha U_h^n, \bar{\partial}_\tau^\alpha U_h^n) + (\nabla U_h^n, \bar{\partial}_\tau^\alpha U_h^n) &= (U_h^n \nabla V_h^n, \bar{\partial}_\tau^\alpha \nabla U_h^n) \\ &\le \|\nabla V_h^n\|_{L^\infty(\Omega)}\|U_h^n\|\|\bar{\partial}_\tau^\alpha \nabla U_h^n\|. \end{aligned} \tag{3.7}$$

By the definition (2.4) and (2.6), we have

$$\begin{aligned} \|\bar{\partial}_\tau^\alpha \nabla U_h^n\| &= \|\sum_{k=1}^{n} a_{n,k}\nabla_\tau \nabla U_h^k\| \\ &= \|a_{n,n}\nabla U_h^n - \sum_{k=1}^{n-1}(a_{n,k+1} - a_{n,k})\nabla U_h^k - a_{n,1}\nabla U_h^0\| \\ &\le a_{n,n}\|\nabla U_h^n\|_{L^\infty(\Omega)}| + \sum_{k=1}^{n-1}(a_{n,k+1} - a_{n,k})\|\nabla U_h^k\| + a_{n,1}\|\nabla U_h^0\| \\ &\le \left(a_{n,n} + \sum_{k=1}^{n-1}(a_{n,k+1} - a_{n,k}) + a_{n,1}\right)\max_{0\le k\le n}\|\nabla U_h^k\| \\ &= 2a_{n,n}\max_{0\le k\le n}\|\nabla U_h^k\| = \frac{2\tau_n^{-\alpha}}{\Gamma(2-\alpha)}\max_{0\le k\le n}\|\nabla U_h^k\|. \end{aligned} \tag{3.8}$$

By using Poincaré inequality in (3.7) and (2.8), we can get

$$\bar{\partial}_\tau^\alpha \|\nabla U_h^n\|^2 \le 4a_{n,n}M\max_{0\le k\le n}\|\nabla U_h^k\|^2. \tag{3.9}$$

Thus, using the fractional Grönwall inequality yields

$$\max_{0\le k\le n}\|\nabla U_h^k\| \le 2E_\alpha(8a_{n,n}Mt_n^\alpha)\|\nabla U_h^0\|. \tag{3.10}$$

Taking $w_h = -\Delta V_h^n$ in the second equation of the fully discrete scheme (2.22), we can have

$$(\bar{\partial}_\tau^\alpha \nabla V_h^n, \nabla V_h^n) + (\Delta V_h^n, \Delta V_h^n) + (\nabla V_h^n, \nabla V_h^n) = (\nabla U_h^n, \nabla V_h^n). \tag{3.11}$$

Then, using Young's inequality and (2.8), we get

$$\bar{\partial}_\tau^\alpha \|\nabla V_h^n\|^2 \le 2\|\nabla U_h^n\|\|\nabla V_h^n\| \le \|\nabla U_h^n\|^2 + \|\nabla V_h^n\|^2. \tag{3.12}$$

Therefore, by discrete fractional Grönwall inequality (2.12), we get

$$\|\nabla V_h^n\| \le 2E_\alpha(2t_n^\alpha)\left(\|\nabla V_h^0\| + \max_{1\le j\le n}\|\nabla U_h^j\|\right). \tag{3.13}$$

Together with (3.10), we can derive (3.2). □

4. α-robust error analysis of the L1/finite element scheme

In this section, we shall consider the error estimates of the L1/finite element scheme. Firstly, We begin by discussing the spatial error estimates of the fully discrete scheme (2.22) in both $L^2(\Omega)$ and $H^1(\Omega)$ norms.

Theorem 4.1. *Let $U^n,\ V^n \in H^{k+1}(\Omega) \cap H_0^1(\Omega)$ be the solution of the semidiscrete scheme* (2.14)*, and $U_h^n, V_h^n \in V_h$ be the solution to the fully discrete scheme* (2.22)*. Then, for $1 \le n \le N$, the following error estimates hold:*

$$\|U^n - U_h^n\| + \|V^n - V_h^n\| \le Ch^{k+1}; \tag{4.1}$$

$$\|U^n - U_h^n\|_1 + \|V^n - V_h^n\|_1 \le Ch^k, \tag{4.2}$$

where C is an α-robust constant.

Proof. Denoting that

$$U^n - U_h^n = U^n - R_hU^n + R_hU^n - U_h^n = \theta_h^n + \eta_h^n,$$

$$V^n - V_h^n = V^n - R_hV^n + R_hV^n - V_h^n = \rho_h^n + \beta_h^n,$$

subtracting the first equation in the fully discrete scheme (2.22) from the first equation in the semidiscrete scheme (2.14) yields

$$\begin{aligned}(\bar{\partial}_\tau^\alpha \eta_h^n, w_h) + (\nabla\eta_h^n, \nabla w_h) &= (U^n\nabla V^n - U_h^n\nabla V_h^n, \nabla w_h) - (\bar{\partial}_\tau^\alpha\theta_h^n, w_h)\\ &\le \frac{M}{\varepsilon}\|U^n - U_h^n\|^2 + \varepsilon\|\nabla w_h\|^2 + \|\bar{\partial}_\tau^\alpha\theta_h^n\|\|w_h\|\\ &\le \frac{M}{\varepsilon}(\|\eta_h^n\|^2 + \|\theta_h^n\|^2) + \varepsilon\|\nabla w_h\|^2 + \|\bar{\partial}_\tau^\alpha\theta_h^n\|\|w_h\|.\end{aligned} \tag{4.3}$$

By the interpolation estimation (2.21) and the definition of (2.4), we have

$$\|\bar{\partial}_\tau^\alpha\theta_h^n\| \le 2a_{n,n}Ch^{k+1}.$$

Let $w_h = \eta_h^n$ in (4.3), we can obtain that

$$\bar{\partial}_\tau^\alpha\|\eta_h^n\|^2 \le \left(1 + \frac{2M}{\varepsilon}\right)\|\eta_h^n\|^2 + \left(4a_{n,n} + \frac{2M}{\varepsilon}\right)Ch^{2(k+1)}.$$

Also, we have $\|\eta_h^0\| = 0$. So, we use the fractional Grönwall inequality to get

$$\|\eta_h^n\| \le 2E_\alpha\left(2\left(1 + \frac{2M}{\varepsilon}t_n^\alpha\right)\right)\left(4a_{n,n} + \frac{2M}{\varepsilon}\right)Ch^{k+1}. \tag{4.4}$$

Similarly, subtracting the second equation in the fully discrete scheme (2.22) from the second equation in the semidiscrete scheme (2.14) yields

$$(\bar{\partial}_\tau^\alpha\beta_h^n, w_h) + (\nabla\beta_h^n, \nabla w_h) = -(\beta_h^n + \rho_h^n, w_h) - (\bar{\partial}_\tau^\alpha\rho_h^n, w_h) + (\theta_h^n + \eta_h^n, w_h). \tag{4.5}$$

Let $w_h^n = \beta_h^n$. Then, using Young's inequality and the interpolation estimates (2.21) to get

$$\begin{aligned}(\bar{\partial}_\tau^\alpha \beta_h^n, \beta_h^n) &\le \|\beta_h^n\|^2 + \|\rho_h^n\|\|\beta_h^n\| + \|\bar{\partial}_\tau^\alpha \rho_h^n\|\|\beta_h^n\| + \|\theta_h^n\|\|\beta_h^n\| + \|\eta_h^n\|\|\beta_h^n\| \\ &\le \frac{3}{2}\|\beta_h^n\|^2 + \left(2Ch^{k+1} + \|\bar{\partial}_\tau^\alpha \rho_h^n\|\right)\|\beta_h^n\| + \frac{1}{2}\|\eta_h^n\|^2.\end{aligned} \tag{4.6}$$

Similar to (3.8), we have

$$\|\bar{\partial}_\tau^\alpha \rho_h^n\| = \left\| \sum_{i=1}^{n} a_{n,n-i} \nabla_\tau \rho_h^i \right\| \le 2a_{n,n} \max_{1\le i\le n} \|\rho_h^i\| \le 2a_{n,n} Ch^{k+1}. \tag{4.7}$$

Also, $\bar{\partial}_\tau^\alpha \|\beta_h^n\|^2 \le 2(\bar{\partial}_\tau^\alpha \beta_h^n, \beta_h^n)$ and $\|\beta_h^0\| = 0$. Thus, it follows from Lemma 2.1 and (2.11) that

$$\begin{aligned}\|\beta_h^n\| \le& 2E_\alpha(6t_n^\alpha)\left(\|\beta_h^0\| + \max_{1\le i\le n}\sum_{j=1}^{i} P_{i,i-j}\left(2(2+2a_{n,n})Ch^{k+1} + \|\eta_h^j\|\right) + \max_{1\le j\le n}\|\eta_h^j\|\right) \\ \le& 2E_\alpha(6t_n^\alpha)\left(\max_{1\le i\le n}\left\{\frac{11(2+2a_{n,n})t_i^\alpha}{2\Gamma(1+\alpha)}Ch^{k+1} + \frac{11t_i^\alpha}{4\Gamma(1+\alpha)}\max_{1\le j\le i}\|\eta_h^j\|\right\}\right. \\ &\left. + \max_{1\le j\le n}\|\eta_h^j\|\right) \\ \le& 2E_\alpha(6t_n^\alpha)\left(\frac{11(2+2a_{n,n})t_n^\alpha}{2\Gamma(1+\alpha)}Ch^{k+1} + \left(1 + \frac{11t_n^\alpha}{4\Gamma(1+\alpha)}\right)\max_{1\le j\le n}\|\eta_h^j\|\right) \\ \le& C_1\left(h^{k+1} + \max_{1\le j\le n}\|\eta_h^j\|\right),\end{aligned} \tag{4.8}$$

where

$$C_1 = \max\left\{\frac{11(1+2a_{n,n})E_\alpha(6t_n^\alpha)t_n^\alpha}{\Gamma(1+\alpha)}C,\ 2E_\alpha(6t_n^\alpha)\left(1 + \frac{11t_n^\alpha}{4\Gamma(1+\alpha)}\right)\right\}.$$

By using the triangle inequality, (4.4) and the interpolation error (2.21), we can obtain (4.1).

Incorporate $w_h = \bar{\partial}_\tau^\alpha \eta_h^n$ into the first equation of (2.22) and (2.14), then subtract the two equations to get

$$\begin{aligned}(\bar{\partial}_\tau^\alpha \eta_h^n, \bar{\partial}_\tau^\alpha \eta_h^n) + (\nabla\eta_h^n, \bar{\partial}_\tau^\alpha \nabla\eta_h^n) &= (U^n\nabla V^n - U_h^n \nabla V_h^n, \bar{\partial}_\tau^\alpha \nabla\eta_h^n) - (\bar{\partial}_\tau^\alpha \theta_h^n, \bar{\partial}_\tau^\alpha \eta_h^n) \\ &\le M(\|\eta_h^n\| + \|\theta_h^n\|)\|\bar{\partial}_\tau^\alpha \nabla\eta_h^n\| + \|\bar{\partial}_\tau^\alpha \theta_h^n\|\|\bar{\partial}_\tau^\alpha \eta_h^n\|.\end{aligned} \tag{4.9}$$

This leads to

$$\|\bar{\partial}_\tau^\alpha \nabla\eta_h^n\| \le 2a_{n,n}\max_{0\le j\le n}\|\nabla\eta_h^j\|, \quad \|\bar{\partial}_\tau^\alpha \theta_h^n\|\| \le 2a_{n,n}Ch^{k+1}.$$

Based on (2.8) and (2.21), we have

$$\begin{aligned}\bar{\partial}_\tau^\alpha \|\nabla\eta_h^n\|^2 &\le 4a_{n,n}M\|\eta_h^n\|\max_{0\le j\le n}\|\nabla\eta_h^j\| + 4a_{n,n}MCh^k\max_{0\le j\le n}\|\nabla\eta_h^j\| + 8a_{n,n}^2Ch^{k+1}\max_{0\le j\le n}\|\eta_h^j\| \\ &\le 4a_{n,n}M\max_{0\le j\le n}\|\nabla\eta_h^j\|^2 + 4(a_{n,n}M + 2a_{n,n}^2)Ch^k\max_{0\le j\le n}\|\nabla\eta_h^j\|.\end{aligned}$$

By applying the fractional Gronwall inequality, $\|\nabla\eta_h^0\| = 0$, and (2.8), we have

$$\max_{0\le j\le n}\|\nabla\eta_h^j\| \le 2E_\alpha(8a_{n,n}Mt_n^\alpha)\frac{11t_n^\alpha}{\Gamma(1+\alpha)}(a_{n,n}M + 2a_{n,n}^2)Ch^k. \tag{4.10}$$

Let $w_h = -\Delta\beta_h^n$ in the Eq(4.5), then use Young's inequality and interpolation estimation (2.21) to get

$$\begin{aligned}(\bar{\partial}_\tau^\alpha \nabla\beta_h^n, \nabla\beta_h^n) \leq & \|\nabla\beta_h^n\|^2 + \|\nabla\rho_h^n\|\|\nabla\beta_h^n\| + \|\bar{\partial}_\tau^\alpha \nabla\rho_h^n\|\|\nabla\beta_h^n\| \\ & + \|\nabla\theta_h^n\|\|\nabla\beta_h^n\| + \|\nabla\eta_h^n\|\|\nabla\beta_h^n\| \\ \leq & \frac{3}{2}\|\nabla\beta_h^n\|^2 + \left(2C_\Omega h^k + \|\bar{\partial}_\tau^\alpha \nabla\rho_h^n\|\right)\|\nabla\beta_h^n\| + \frac{1}{2}\|\nabla\eta_h^n\|^2.\end{aligned} \tag{4.11}$$

By (3.8) and (2.21), we can get

$$\|\bar{\partial}_\tau^\alpha \nabla\rho_h^n\| \leq 2a_{n,n}Ch^k.$$

Then, referring to the deduction of (4.8), it can be concluded that

$$\|\nabla\beta_h^n\| \leq C_1\left(h^k + \max_{1\leq j\leq n}\|\nabla\eta_h^j\|\right). \tag{4.12}$$

Finally, the triangle inequality and (4.10) can be used to prove (4.2). □

Assume that

$$|\partial_t^l u(t)| \leq C(1 + t^{\alpha-l}) \quad \text{for } l = 0, 1, 2.$$
$$|\partial_t^l v(t)| \leq C(1 + t^{\alpha-l}) \quad \text{for } l = 0, 1, 2.$$

Based on the above spatial error results, we further discuss the space-time error estimates of fully discrete schemes (2.22).

Theorem 4.2. *Assume that $u(x,t)$, $v(x,t)$ are the weak solution of problem* (2.2)*, Then, for $n = 0, 1, 2, \ldots, N$, the fully discrete scheme* (2.22) *satisfies*

$$\|u(t_n) - U_h^n\| + \|v(t_n) - V_h^n\| \leq C\left(N^{-min\{2-\alpha,r\alpha\}} + h^{k+1}\right), \tag{4.13}$$
$$\|u(t_n) - U_h^n\|_1 + \|v(t_n) - V_h^n\|_1 \leq C\left(N^{-min\{2-\alpha,r\alpha\}} + h^{k}\right), \tag{4.14}$$

where C is an α-robust constant.

Proof. Define

$$E_u^n = u(t_n) - U^n, \quad E_v^n = v(t_n) - V^n.$$

Subtract the second equation of the the weak form (2.2) and the second equation of the semidiscrete scheme (2.14) to yield

$$\begin{aligned}(\bar{\partial}_\tau^\alpha E_u^n, w) + (\nabla E_u^n, \nabla w) &= (u^n\nabla v^n - U^n\nabla V^n, \nabla w) + (\bar{\partial}_\tau^\alpha u^n - \partial_t^\alpha u^n), w) \\ &\leq M\|E_u^n\|\|\nabla w\| + (\bar{\partial}_\tau^\alpha u^n - \partial_t^\alpha u^n), w).\end{aligned} \tag{4.15}$$

Let $w = E_u^n$ in the above equation, and using the Young's inequality, we have

$$\bar{\partial}_\tau^\alpha\|E_u^n\|^2 + 2\|\nabla E_u^n\|^2 \leq \frac{M}{\varepsilon}\|E_u^n\|^2 + \varepsilon\|\nabla E_u^n\|^2 + 2\|\bar{\partial}_\tau^\alpha u^n - \partial_t^\alpha u^n)\|\|E_u^n\|.$$

Thus, by Lemma 2.1, $E_u^0 = 0$, and the error (2.7), we obtain that

$$\|E_u^n\| \leq 2E_\alpha\left(\frac{2M}{\varepsilon}t_n^\alpha\right)\frac{11t_n^\alpha}{\Gamma(1+\alpha)}CN^{\min\{2-\alpha,r\alpha\}}. \tag{4.16}$$

Subtract the second equation of the the weak form (2.2) and the second equation of the semidiscrete scheme (2.14) to obtain

$$(\bar{\partial}_\tau^\alpha E_v^n, w_h) + (\nabla E_v^n, \nabla w_h) = -(E_v^n, w_h) + (\bar{\partial}_\tau^\alpha v(t_n) - \partial_t^\alpha v(t_n), w_h) + (E_u^n, w_h). \tag{4.17}$$

Let $w_h = E_v^n$ in (4.17). We then apply Young's inequality, (2.8) and (2.7) to get

$$\bar{\partial}_\tau^\alpha \|E_v^n\|^2 \le 3\|E_v^n\|^2 + \|\bar{\partial}_\tau^\alpha v(t_n) - \partial_t^\alpha v(t_n)\|\|E_v^n\| + \|E_u^n\|^2. \tag{4.18}$$

It follows from (2.11) and Lemma 2.1 that

$$\begin{aligned}
\|E_v^n\| \le & 2E_\alpha(6t_n^\alpha)\left(\|E_v^0\| + \max_{1\le k\le n}\sum_{j=1}^{k} P_{k,k-j}\left(\|\bar{\partial}_\tau^\alpha v(t_n) - \partial_t^\alpha v(t_n)\| + \|E_u^j\|\right) + \max_{1\le j\le n}\|E_u^j\|\right) \\
\le & 2E_\alpha(6t_n^\alpha)\left(\frac{11t_n^\alpha}{4\Gamma(1+\alpha)}CN^{-\min\{2-\alpha,r\alpha\}} + \left(1 + \frac{11t_n^\alpha}{4\Gamma(1+\alpha)}\right)\max_{0\le j\le n}\|E_u^j\|\right) \\
\le & C_2\left(N^{-\min\{2-\alpha,r\alpha\}} + \max_{0\le j\le n}\|E_u^j\|\right),
\end{aligned} \tag{4.19}$$

where

$$C_2 = \max\left\{\frac{11E_\alpha(6t_n^\alpha)t_n^\alpha}{2\Gamma(1+\alpha)}C, 2E_\alpha(6t_n^\alpha)\left(1 + \frac{11t_n^\alpha}{4\Gamma(1+\alpha)}\right)\right\}.$$

By the conclusion in (4.1) and (4.16) and using the triangle inequality, we can derive (4.13).

Let $w = -\Delta E_v^n$ in Eq (4.17) and setting $w = \bar{\partial}_\tau^\alpha E_u^n$ in Eq (4.15). Then, we can repeat the above process to get

$$\max_{0\le j\le n}\|\nabla E_u^j\| \le CN^{-\min\{2-\alpha,r\alpha\}} \tag{4.20}$$

and

$$\|\nabla E_v^n\| \le CN^{-\min\{2-\alpha,r\alpha\}}. \tag{4.21}$$

By the conclusion in (4.2), applying the triangle inequality can derive (4.14). □

5. Fast L1/finite element scheme for time-fractional Keller-Segel equations

It is known that the direct algorithm of the L1 scheme (2.4) has the computational cost $O(N^2)$, whose large size is prohibitive for small-time size or long-time simulations. Thus, we shall consider the SOE-based fast nonuniform L1 scheme introduced in [26,27]. Its idea is mainly based on using the sum-of-exponentials (SOE) skill to approximate the convolution kernel $t^{-\alpha}$ over an interval $[\hat{\tau}, T]$ with $\hat{\tau} = \min_{1\le k\le N}\tau_k$, which is given as follows:

Lemma 5.1. *[26] For the given parameters $\alpha \in (0,1)$, tolerance error ϵ, cut-off time step size $\hat{\tau}$, and the final time T, there exist positive points s_i and corresponding positive weights w_i $(i = 1, 2, \cdots, N_{\exp})$ satisfying*

$$\left|t^{-\alpha} - \sum_{i=1}^{N_{\exp}}\omega_i e^{-s_i t}\right| \le \epsilon, \quad \forall t \in [\hat{\tau}, T],$$

where

$$N_{\text{exp}} = O\left(\log\frac{1}{\epsilon}\left(\log\log\frac{1}{\epsilon} + \log\frac{T}{\hat{\tau}}\right) + \log\frac{1}{\hat{\tau}}\left(\log\log\frac{1}{\epsilon} + \log\frac{1}{\hat{\tau}}\right)\right).$$

With the help of above lemma, the SOE-based fast L1 scheme of the Caputo derivative is given [27, 35]:

$$\bar{\partial}_F^{\alpha}\varphi^n = \sum_{k=1}^{n} B_{n-k}^{(n)}\nabla_\tau\varphi^k, \tag{5.1}$$

where

$$B_0^{(n)} = a_{n,n}, \quad B_{n-k}^{(n)} = \frac{1}{\tau_k\Gamma(1-\alpha)}\int_{t_{k-1}}^{t_k}\sum_{i=1}^{N_{\text{exp}}}\omega_i e^{-s_i(t_n-s)}\mathrm{d}s, \quad 1 \le k \le n-1.$$

If $\epsilon \le \epsilon_1 = \min\left\{\frac{1}{3}\omega_{1-\alpha}(T), \alpha\omega_{2-\alpha}(T)\right\}$, then the convolution coefficient $B_{n-k}^{(n)}$ satisfies the following properties [27]:

$$B_k^{(n)} \ge B_{k-1}^{(n)} > 0, \quad B_{n-k}^{(n)} \ge \frac{2}{3}\int_{t_{k-1}}^{t_k}\frac{\omega_{1-\alpha}(t_n-s)}{\tau_k}ds$$

for $2 \le k \le n \le N$. When $|\varphi^{(l)}(t)| \le C(1+t^{\alpha-l})$ for $l = 0, 1, 2$, we shall derive the following truncation error [27]:

$$\left|\partial_t^{\alpha}\varphi(t_n) - \bar{\partial}_F^{\alpha}\varphi^n)\right| \le Cn^{-\min\{2-\alpha, r\alpha\}} + \epsilon, \quad n = 1, 2, \cdots, N. \tag{5.2}$$

In addition, we note the following property [35]:

$$\frac{1}{2}\sum_{k=1}^{n} B_{n-k}^{(n)}\nabla_\tau\|\varphi^k\|^2 \le (\bar{\partial}_F^{\alpha}\varphi^n, \varphi^n). \tag{5.3}$$

Lemma 5.2. *[33] For any nonnegative sequences* $\{\xi^n\}_{n=1}^N$,$\{\eta^n\}_{n=1}^N$,*and* $\{\lambda_k\}_{n=1}^{N-1}$, *there exists a constant* Λ *such that* $\sum_{k=0}^{N-1}\lambda_k \le \Lambda$ *for* $N \ge 1$. *Let the grid function* $\{\varphi^k\}_{k=0}^N$ *satisfy*

$$\bar{\partial}_F^{\alpha}(\varphi^k)^2 \le \sum_{k=1}^{n}\lambda_k(\varphi^k)^2 + \xi^n\varphi^n + (\eta^n)^2. \tag{5.4}$$

If the maximum step-size $\tau^* \le (2\Gamma(2-\alpha)\Lambda)^{-1/\alpha}$, *it holds that, for* $1 \le n \le N$,

$$\varphi_n \le C\left(\varphi_0 + \max_{1\le j\le n}\{t_j^{\alpha}(\xi^j + \eta^j)\} + \max_{1\le j\le n}\{\eta^j\}\right), \tag{5.5}$$

where C is α*-robust.*

Next, by replacing the L1 scheme in the fully discrete scheme (2.22) with the above fast L1 scheme (5.1), we can derive a fast L1 finite element scheme: Find $(U_h^n, V_h^n) \in S_h \times S_h$, for $n = 1, 2, \ldots, N$, such that

$$\begin{cases} (\bar{\partial}_F^{\alpha}U_h^n, w_h) + (\nabla U_h^n, \nabla w_h) - (U_h^n\nabla V_h^n, \nabla w_h) = 0, & w_h \in S_h, \\ (\bar{\partial}_F^{\alpha}V_h^n, w_h) + (\nabla V_h^n, \nabla w_h) + (V_h^n, w_h) = (U_h^n, w_h), & w_h \in S_h, \\ U_h^0 = R_h u_0, \ V_h^0 = R_h v_0. \end{cases} \tag{5.6}$$

By observing the properties of the coefficients in the fast L1 scheme (5.1), we can see that they are consistent with the properties of the L1 scheme (2.4). Then, by combining the fractional Grönwall inequality provided in [33], we can similarly derive the stability and error estimation of the fast L1 finite element scheme. The results are as follows.

Theorem 5.1. *For $n = 0, 1, 2, \ldots, N$, the fast L1 scheme* (5.6) *satisfies the following stability results:*

$$\|U_h^n\| + \|V_h^n\| \le C\left(\|U_h^0\| + \|V_h^0\|\right), \tag{5.7}$$

$$\|U_h^n\|_1 + \|V_h^n\|_1 \le C\left(\|U_h^0\|_1 + \|V_h^0\|_1\right), \tag{5.8}$$

where C is an α-robust constant.

Proof. By Lemma 5.2 and (5.3), similar to Theorem 3.1, we can obtain the above conclusion. □

Theorem 5.2. *Assume that $(u(x,t), v(x,t)) \in C^2\left([0,T]; L^2(\Omega)\right) \cap C^1\left([0,T]; H^{k+1}(\Omega)\right)$ are the weak solution of problem* (2.2)*. Then, for $n = 0, 1, 2, \ldots, N$, the fast L1 discrete scheme* (5.6) *satisfies*

$$\|u(t_n) - U_h^n\| + \|v(t_n) - V_h^n\| \le C\left(N^{-min\{2-\alpha, r\alpha\}} + h^{k+1} + \epsilon\right), \tag{5.9}$$

$$\|u(t_n) - U_h^n\|_1 + \|v(t_n) - V_h^n\|_1 \le C\left(N^{-min\{2-\alpha, r\alpha\}} + h^{k} + \epsilon\right), \tag{5.10}$$

where C is an α-robust constant.

Proof. According to the deduction of Theorem 4.1, we have

$$\|U^n - U_h^n\| + \|V^n - V_h^n\| \le Ch^{k+1};$$
$$\|U^n - U_h^n\|_1 + \|V^n - V_h^n\|_1 \le Ch^{k}.$$

Then, by Lemma 5.2, (5.2) and (5.3), similar to the deduction of Theorem 4.2, we can obtain the above conclusion. □

6. Numerical example

In this section, we shall present a numerical example to verify the effectiveness of our numerical scheme and the reliability of our theoretical results. To derive the numerical solution, we adapt the L1 or fast L1 scheme to approximate the time Caputo fractional derivative with the mesh parameter $r \ge (2-\alpha)/\alpha$, and apply the linear finite element to discrete the spatial direction. Moreover, we choose the tolerance error $\epsilon = 10^{-12}$ and the cut-off time $\hat{\tau} = 10^{-12}$ to speed up the convolution computation of the L1 scheme. At each time level, the nonlinear algebraic system is solved by using fixed-point algorithms with the termination error 10^{-12}. For simplicity, we define

$$\|E_u\| = \max_{1\le n\le N} \|u(t_n) - U_h^n\|, \quad \|E_u\|_1 = \max_{1\le n\le N} \|u(t_n) - U_h^n\|_1,$$

$$\|E_v\| = \max_{1\le n\le N} \|v(t_n) - V_h^n\|, \quad \|E_v\|_1 = \max_{1\le n\le N} \|v(t_n) - V_h^n\|_1.$$

Then, we consider the following example.

Example 6.1. *Assume the domain* $\Omega = (0,1)^2$*, and the final time* $T = 1 \times 10^{-6}$*. Then, we consider the following time-fractional order KS equations:*

$$\begin{cases} \partial_t^\alpha u - \Delta u + \nabla \cdot (u \nabla v) = f, & \mathbf{x} \in \Omega,\ 0 < t < T, \\ \partial_t^\alpha v - \Delta v + v - u = g, & \mathbf{x} \in \Omega,\ 0 < t < T, \end{cases} \tag{6.1}$$

and the exact solutions (u, v) *are given by*

$$u = 4\pi(t^2 + t^\alpha)\sin(\pi x)\sin(\pi y), \quad v = (t^2 + t^\alpha)\sin(\pi x)\sin(\pi y). \tag{6.2}$$

Thus, the right-hand f *and* g *are determined from the choice for* u *and* v*.*

Next, we fix the time step $N = 100$ and space mesh size $h = 1/32$. We see that the errors change little as $\alpha \to 1^-$ in Table 1, which implies that our method is α-robust. In Figure 1, it shows that the numerical solution is consistent with the exact solution.

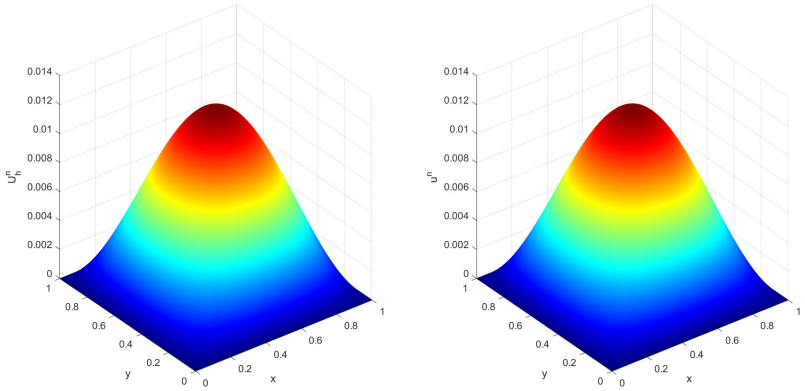

(a) Left: Numerical solution U_h^n, Right: Exact solution u^n.

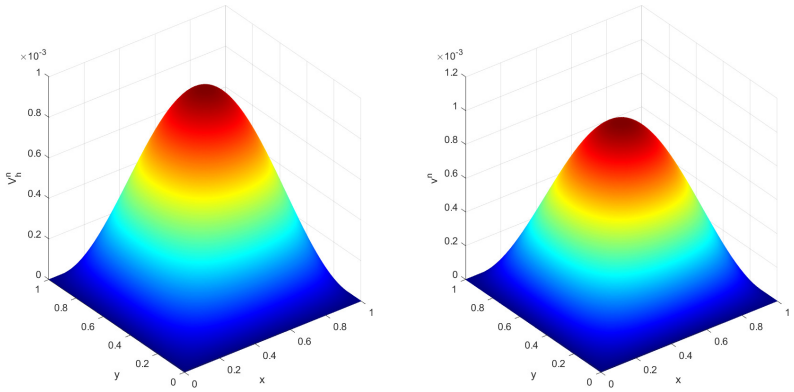

(b) Left: Numerical solution V_h^n, Right: Exact solution v^n.

Figure 1. Comparison figure of the exact solution and numerical solution for $N = 100,\ h = 1/64,\ \alpha = 0.5, r = 2/\alpha$.

Table 1. α-robustness test with $N = 100,\ h = 1/32$, and $r = 2/\alpha$.

Method	Error	$\alpha = 0.90$	$\alpha = 0.95$	$\alpha = 0.99$	$\alpha = 0.999$
L1/FEM scheme	$\|\|E_u\|\|$	4.076×10^{-8}	1.512×10^{-8}	3.734×10^{-9}	2.692×10^{-9}
	$\|\|E_v\|\|$	3.244×10^{-9}	1.203×10^{-9}	2.971×10^{-10}	2.142×10^{-10}
	$\|\|E_u\|\|_1$	5.471×10^{-6}	2.743×10^{-6}	1.579×10^{-6}	1.395×10^{-6}
	$\|\|E_v\|\|_1$	4.354×10^{-7}	2.182×10^{-7}	1.257×10^{-7}	1.110×10^{-7}
Fast L1/FEM scheme	$\|\|E_u\|\|$	4.076×10^{-8}	1.512×10^{-8}	3.734×10^{-9}	2.692×10^{-9}
	$\|\|E_v\|\|$	3.244×10^{-9}	1.203×10^{-9}	2.971×10^{-10}	2.142×10^{-10}
	$\|\|E_u\|\|_1$	5.471×10^{-6}	2.743×10^{-6}	1.579×10^{-6}	1.395×10^{-6}
	$\|\|E_v\|\|_1$	4.354×10^{-7}	2.182×10^{-7}	1.257×10^{-7}	1.110×10^{-7}

Table 2. The spatial error convergence orders of L1/FEM for $N = 500$ and $r = 2/\alpha$.

α	h	$\|\|E_u\|\|$	Rate	$\|\|E_u\|\|_1$	Rate	$\|\|E_v\|\|$	Rate	$\|\|E_v\|\|_1$	Rate
0.4	1/4	1.384×10^{-3}	–	4.523×10^{-2}	–	1.105×10^{-4}	–	3.597×10^{-3}	–
	1/8	2.745×10^{-4}	2.3345	2.209×10^{-2}	1.0342	2.192×10^{-5}	2.3335	1.757×10^{-3}	1.0335
	1/16	6.324×10^{-5}	2.1179	1.095×10^{-2}	1.0129	4.996×10^{-6}	2.1333	8.710×10^{-4}	1.0126
	1/32	1.677×10^{-5}	1.9151	5.459×10^{-3}	1.0035	1.229×10^{-6}	2.0236	4.340×10^{-4}	1.0035
0.6	1/4	8.227×10^{-5}	–	2.928×10^{-3}	–	6.547×10^{-6}	–	2.330×10^{-4}	–
	1/8	1.498×10^{-5}	2.4570	1.410×10^{-3}	1.0545	1.192×10^{-6}	2.4569	1.122×10^{-4}	1.0545
	1/16	3.061×10^{-6}	2.2916	6.938×10^{-4}	1.0226	2.436×10^{-7}	2.2915	5.521×10^{-5}	1.0226
	1/32	7.007×10^{-7}	2.1270	3.450×10^{-4}	1.0080	5.576×10^{-8}	2.1270	2.745×10^{-5}	1.0080
0.8	1/4	5.187×10^{-6}	–	1.851×10^{-4}	–	4.128×10^{-7}	–	1.473×10^{-5}	–
	1/8	9.440×10^{-7}	2.4581	8.907×10^{-5}	1.0553	7.512×10^{-8}	2.4581	7.088×10^{-6}	1.0553
	1/16	1.926×10^{-7}	2.2927	4.384×10^{-5}	1.0227	1.533×10^{-8}	2.2927	3.489×10^{-6}	1.0227
	1/32	4.814×10^{-8}	2.0006	2.179×10^{-5}	1.0083	3.831×10^{-9}	2.0005	1.734×10^{-6}	1.0083

Table 3. The spatial error convergence orders of fast L1/FEM for $N = 500$ and $r = 2/\alpha$.

α	h	$\|\|E_u\|\|$	Rate	$\|\|E_u\|\|_1$	Rate	$\|\|E_v\|\|$	Rate	$\|\|E_v\|\|_1$	Rate
0.4	1/4	1.385×10^{-3}	–	4.523×10^{-2}	–	1.105×10^{-4}	–	3.597×10^{-3}	–
	1/8	2.745×10^{-4}	2.3345	2.209×10^{-2}	1.0342	2.192×10^{-5}	2.3335	1.757×10^{-3}	1.0335
	1/16	6.325×10^{-5}	2.1179	1.095×10^{-2}	1.0129	4.996×10^{-6}	2.1333	8.710×10^{-4}	1.0126
	1/32	1.677×10^{-5}	1.9151	5.459×10^{-3}	1.0035	1.229×10^{-6}	2.0236	4.345×10^{-4}	1.0035
0.6	1/4	8.227×10^{-5}	–	2.928×10^{-3}	–	6.547×10^{-6}	–	2.330×10^{-4}	–
	1/8	1.498×10^{-5}	2.4570	1.410×10^{-3}	1.0545	1.192×10^{-6}	2.4569	1.122×10^{-4}	1.0545
	1/16	3.061×10^{-6}	2.2916	6.938×10^{-4}	1.0226	2.436×10^{-7}	2.2915	5.521×10^{-5}	1.0226
	1/32	7.007×10^{-7}	2.1270	3.450×10^{-4}	1.0080	5.576×10^{-8}	2.1270	2.745×10^{-5}	1.0080
0.8	1/4	5.187×10^{-6}	–	1.851×10^{-4}	–	4.128×10^{-7}	–	1.473×10^{-5}	–
	1/8	9.440×10^{-7}	2.4581	8.907×10^{-5}	1.0553	7.512×10^{-8}	2.4581	7.088×10^{-6}	1.0553
	1/16	1.927×10^{-7}	2.2927	4.384×10^{-5}	1.0227	1.533×10^{-8}	2.2927	3.489×10^{-6}	1.0227
	1/32	4.815×10^{-8}	2.0006	2.179×10^{-5}	1.0083	3.831×10^{-9}	2.0005	1.734×10^{-6}	1.0083

Let the time step $N = 500$. We shall give the spatial error convergence orders of the L1/FEM scheme and fast L1/FEM scheme in Tables 2 and 3 for $\alpha = 0.4, 0.6, 0.8$, respectively. It shown that the L^2-error convergence order is two and the H^1-error convergence order is one, and we know that the error estimate of these two methods are almost identical. We also fixed the space mesh size $h = 1/100$, the time error order shown in Table 4 is approximately $O(2 - \alpha)$. However, we can know that the time convergence order is only $O(\alpha)$ when we use a uniform time mesh; see Table 5. Compared to the grade mesh, this result is not optimal. Thus, the above numerical results are consistent with the conclusions of Theorems 4.2 and 5.2. This also indicates that our method is efficient.

Table 4. The time error convergence orders of L1/FEM and fast L1/FEM with $h = 1/100$ and $r = 2/\alpha$.

α	N	L1/FEM scheme				Fast L1/FEM scheme			
		$\|\|E_u\|\|$	Rate	$\|\|E_v\|\|$	Rate	$\|\|E_u\|\|$	Rate	$\|\|E_v\|\|$	Rate
0.4	8	5.474×10^{-4}	–	4.529×10^{-5}	–	5.474×10^{-4}	–	4.529×10^{-5}	–
	16	1.954×10^{-4}	1.4859	1.603×10^{-5}	1.4987	1.954×10^{-4}	1.4859	1.603×10^{-5}	1.4987
	32	6.985×10^{-5}	1.4842	5.572×10^{-6}	1.5244	6.985×10^{-5}	1.4842	5.572×10^{-6}	1.5244
	64	2.630×10^{-5}	1.4090	1.936×10^{-6}	1.5248	2.630×10^{-5}	1.4090	1.936×10^{-6}	1.5248
0.6	8	4.522×10^{-5}	–	3.609×10^{-6}	–	4.522×10^{-5}	–	3.609×10^{-6}	–
	16	1.813×10^{-5}	1.3189	1.447×10^{-6}	1.3189	1.813×10^{-5}	1.3189	1.447×10^{-6}	1.3189
	32	7.061×10^{-6}	1.3602	5.635×10^{-7}	1.3603	7.061×10^{-6}	1.3602	5.635×10^{-7}	1.3603
	64	2.718×10^{-6}	1.3771	2.169×10^{-7}	1.3773	2.718×10^{-6}	1.3771	2.169×10^{-7}	1.3773
0.8	8	2.525×10^{-6}	–	2.010×10^{-7}	–	2.525×10^{-6}	–	2.010×10^{-7}	–
	16	1.172×10^{-6}	1.1078	9.327×10^{-8}	1.1078	1.172×10^{-6}	1.1078	9.327×10^{-8}	1.1078
	32	5.265×10^{-7}	1.1543	4.190×10^{-8}	1.1543	5.265×10^{-7}	1.1543	4.190×10^{-8}	1.1543
	64	2.328×10^{-7}	1.1775	1.853×10^{-8}	1.1775	2.328×10^{-7}	1.1775	1.853×10^{-8}	1.1775

Table 5. The time error convergence orders of L1/FEM and fast L1/FEM with $h = 1/100$ and $r = 1$.

α	N	L1/FEM scheme				Fast L1/FEM scheme			
		$\|\|E_u\|\|$	Rate	$\|\|E_v\|\|$	Rate	$\|\|E_u\|\|$	Rate	$\|\|E_v\|\|$	Rate
0.4	8	2.189×10^{-3}	–	1.772×10^{-4}	–	2.189×10^{-3}	–	1.772×10^{-4}	–
	16	1.671×10^{-3}	0.3897	1.348×10^{-4}	0.3954	1.671×10^{-3}	0.38966	1.348×10^{-4}	0.3954
	32	1.274×10^{-3}	0.3921	1.024×10^{-4}	0.3966	1.274×10^{-3}	0.39211	1.024×10^{-4}	0.3966
	64	9.692×10^{-4}	0.3940	7.772×10^{-5}	0.3974	9.692×10^{-4}	0.39398	7.772×10^{-5}	0.3974
0.6	8	9.380×10^{-5}	–	7.470×10^{-6}	–	9.380×10^{-5}	–	7.469×10^{-6}	–
	16	6.191×10^{-5}	0.5994	4.929×10^{-6}	0.5997	6.191×10^{-5}	0.59938	4.929×10^{-6}	0.5997
	32	4.086×10^{-5}	0.5996	3.252×10^{-6}	0.5998	4.086×10^{-5}	0.59959	3.252×10^{-6}	0.5998
	64	2.696×10^{-5}	0.5997	2.146×10^{-6}	0.5999	2.696×10^{-5}	0.59973	2.146×10^{-6}	0.5999
0.8	8	3.049×10^{-6}	–	2.426×10^{-7}	–	3.049×10^{-6}	–	2.426×10^{-7}	–
	16	1.751×10^{-6}	0.7999	1.394×10^{-7}	0.7999	1.751×10^{-6}	0.79989	1.394×10^{-7}	0.7999
	32	1.006×10^{-6}	0.7999	8.004×10^{-8}	0.7999	1.006×10^{-6}	0.79994	8.004×10^{-8}	0.7999
	64	5.777×10^{-7}	0.7999	4.597×10^{-8}	0.7999	5.777×10^{-7}	0.79996	4.597×10^{-8}	0.7999

Finally, we provide the computation time for both the L1/FEM scheme and fast L1/FEM scheme in Table 6. Through comparison, we can see that the fast algorithm can greatly save computational cost.

Table 6. The computing time of the L1/FEM and the fast L1/FEM scheme with $h = 1/16$, $\alpha = 0.5$, and $r = 2/\alpha$.

N	2000	4000	6000	8000	10000
L1/FEM scheme	21.0041 s	60.5883 s	119.1214 s	194.54 s	287.6419 s
Fast L1/FEM scheme	12.9594 s	27.7864 s	41.4982 s	55.8147 s	71.7922 s

7. Conclusions

This work presents an L1/FEM scheme and fast L1/FEM scheme for solving time-fractional KS equations with weakly singular solutions. Based on an improved fractional Grönwall inequality and the boundedness of $\nabla v, \nabla V$, and ∇V_h^n, we establish the stability and the α-robust error estimates for numerical schemes under both $L^2(\Omega)$ and $H^1(\Omega)$ norms. According to theoretical results, the error convergence order of our numerical scheme is optimal. Finally, a numerical example is presented to illustrate the reliability of our algorithms and the correctness of our theoretical results. However, there are still some minor flaws here, such as the small final time of our numerical simulation. For this problem, we will further study the blow-up of the numerical solution to derive long-term numerical simulations.

Use of AI tools declaration

The authors declare they have not used Artificial Intelligence (AI) tools in the creation of this article.

Acknowledgments

Qingfeng Li is supported by the Educational Commission Science Program of Jiangxi Province (GJJ2201245) and the Natural Science Foundation of Jiangxi Province (20242BAB20007).

Conflict of interest

The authors declare there are no conflicts of interest.

References

1. E. F. Keller, L. A. Segel, Initiation of slime mold aggregation viewed as an instability, *J. Theor. Biol.*, **26** (1970), 399–415. https://doi.org/10.1016/0022-5193(70)90092-5
2. E. F. Keller, L. A. Segel, Traveling bands of chemotactic bacteria: A theoretical analysis, *J. Theor. Biol.*, **30** (1971), 235–248. https://doi.org/10.1016/0022-5193(71)90051-8
3. M. Winkler, Chemotaxis with logistic source: Very weak global solutions and their boundedness properties, *J. Math. Anal. Appl.*, **348** (2008), 708–729. https://doi.org/10.1016/j.jmaa.2008.07.071

4. J. Xu, H. Fu, A decoupled linear, mass-conservative block-centered finite difference method for the Keller-Segel chemotaxis system, *J. Comput. Phys.*, **526** (2025), 113775. https://doi.org/10.1016/j.jcp.2025.113775
5. J. Hu, X. Zhang, Positivity-preserving and energy-dissipative finite difference schemes for the Fokker-Planck and Keller-Segel equations, *IMA J. Numer. Anal.*, **43** (2023), 1450–1484. https://doi.org/10.1093/imanum/drac014
6. G. Zhou, N. Saito, Finite volume methods for a Keller-Segel system: Discrete energy, error estimates and numerical blow-up analysis, *Numer. Math.*, **135** (2017), 265–311. https://doi.org/10.1007/s00211-016-0793-2
7. M. Sulman, T. Nguyen, A positivity preserving moving mesh finite element method for the Keller-Segel chemotaxis model, *J. Sci. Comput.*, **80** (2019), 649–666. https://doi.org/10.1007/s10915-019-00951-0
8. K. Wang, E. Liu, X. Feng, Optimal error estimate of unconditionally positivity-preserving, mass-conserving and energy stable method for the Keller-Segel chemotaxis model, *Math. Comput.*, **94** (2025), 2761–2793. https://doi.org/10.1090/mcom/4041
9. J. Shen, J. Xu, Unconditionally bound preserving and energy dissipative schemes for a class of Keller-Segel equations, *SIAM J. Numer. Anal.*, **58** (2020), 1674–1695. https://doi.org/10.1137/19M1246705
10. R. Metzler, J. Klafter, The random walk's guide to anomalous diffusion: A fractional dynamics approach, *Phys. Rep.*, **339** (2000), 1–77. https://doi.org/10.1016/S0370-1573(00)00070-3
11. F. A. Rihan, Numerical modeling of fractional-order biological systems, *Abstr. Appl. Anal.*, **2013** (2013), 816803. https://doi.org/10.1155/2013/816803
12. L. Li, J. Liu, Some compactness criteria for weak solutions of time fractional PDEs, *SIAM J. Math. Anal.*, **50** (2018), 3963–3995. https://doi.org/10.1137/17M1145549
13. Y. Zhou, J. Manimaran, L. Shangerganesh, A. Debbouche, Weakness and Mittag-Leffler stability of solutions for time-fractional Keller-Segel models, *Int. J. Nonlinear Sci. Numer. Simul.*, **19** (2018), 753–761. https://doi.org/10.1515/ijnsns-2018-0035
14. M. Bezerra, C. Cuevas, C. Silva, H. Soto, On the fractional doubly parabolic Keller-Segel system modelling chemotaxis, *Sci. China Math.*, **65** (2022), 1827–1874. https://doi.org/10.1007/s11425-020-1846-x
15. M. Costa, C. Cuevas, C. Silva, H. Soto, Well-posedness and blow-up of the fractional Keller-Segel model on domains, *Math. Nachr.*, **296** (2023), 5569–5592. https://doi.org/10.1002/mana.202200235
16. A. Slimani, S. Lakhlifa, A. Guesmia, Analytical solution of one-dimensional Keller-Segel equations via new homotopy perturbation method, *Contemp. Math.*, **5** (2024), 1093–1109. https://doi.org/10.37256/CM.5120242604
17. M. Zayernouri, A. Matzavinos, Fractional Adams-Bashforth/Moulton methods: An application to the fractional Keller-Segel chemotaxis system, *J. Comput. Phys.*, **317** (2016), 1–14. https://doi.org/10.1016/j.jcp.2016.04.041

18. K. Sakamoto, M. Yamamoto, Initial value/boundary value problems for fractional diffusion-wave equations and applications to some inverse problems, *J. Math. Anal. Appl.*, **382** (2011), 426–447. https://doi.org/10.1016/j.jmaa.2011.04.058

19. M. Stynes, E. O'Riordan, J. L. Gracia, Error analysis of a finite difference method on graded meshes for a time-fractional diffusion equation, *SIAM J. Numer. Anal.*, **55** (2017), 1057–1079. https://doi.org/10.1137/16M1082329

20. B. Jin, B. Li, Z. Zhou, Numerical analysis of nonlinear subdiffusion equations, *SIAM J. Numer. Anal.*, **56** (2018), 1–23. https://doi.org/10.1137/16M1089320

21. H. Liao, D. Li, J. Zhang, Sharp error estimate of the nonuniform L1 formula for linear reaction-subdiffusion equations, *SIAM J. Numer. Anal.*, **56** (2018), 1112–1133. https://doi.org/10.1137/17M1131829

22. H. Liao, W. McLean, J. Zhang, A discrete Grönwall inequality with applications to numerical schemes for subdiffusion problems, *SIAM J. Numer. Anal.*, **57** (2019), 218–237. https://doi.org/10.1137/16M1175742

23. N. Kopteva, Error analysis of the L1 method on graded and uniform meshes for a fractional-derivative problem in two and three dimensions, *Math. Comput.*, **88** (2019), 2135–2155. https://doi.org/10.1090/mcom/3410

24. N. Kopteva, Error analysis of an L2-type method on graded meshes for a fractional-order parabolic problem, *Math. Comput.*, **90** (2021), 19–40. https://doi.org/10.1090/mcom/3552

25. H. Chen, M. Stynes, Error analysis of a second-order method on fitted meshes for a time-fractional diffusion problem, *J. Sci. Comput.*, **79** (2019), 624–647. https://doi.org/10.1007/s10915-018-0863-y

26. S. Jiang, J. Zhang, Q. Zhang, Z. Zhang, Fast evaluation of the caputo fractional derivative and its applications to fractional diffusion equations, *Commun. Comput. Phys.*, **21** (2017), 650–678. https://doi.org/10.4208/cicp.OA-2016-0136

27. H. Liao, Y. Yan, J. Zhang, Unconditional convergence of a fast two-level linearized algorithm for semilinear subdiffusion equations, *J. Sci. Comput.*, **80** (2019), 1–25. https://doi.org/10.1007/s10915-019-00927-0

28. C. Huang, M. Stynes, A sharp α-robust $\mathrm{L}^{\infty}(H^1)$ error bound for a time-fractional Allen-Cahn problem discretised by the Alikhanov L2-1_{σ} scheme and a standard FEM, *J. Sci. Comput.*, **91** (2022), 43. https://doi.org/10.1007/s10915-022-01810-1

29. H. Chen, M. Stynes, Blow-up of error estimates in time-fractional initial-boundary value problems, *IMA J. Numer. Anal.*, **41** (2021), 974–997. https://doi.org/10.1093/imanum/draa015

30. Z. Sheng, Y. Liu, Y. Li, Finite element method combined with time graded meshes for the time-fractional coupled Burgers' equations, *J. Appl. Math. Comput.*, **70** (2024), 513–533. https://doi.org/10.1007/s12190-023-01969-2

31. C. Huang, M. Stynes, Optimal spatial H^1-norm analysis of a finite element method for a time-fractional diffusion equation, *J. Comput. Appl. Math.*, **367** (2020), 112435. https://doi.org/10.1016/j.cam.2019.112435

32. C. Huang, M. Stynes, α-robust error analysis of a mixed finite element method for a time-fractional biharmonic equation, *Numer. Algorithms*, **87** (2021), 1749–1766. https://doi.org/10.1007/s11075-020-01036-y

33. Z. Tan, α-robust analysis of fast and novel two-grid fem with nonuniform L1 scheme for semilinear time-fractional variable coefficient diffusion equations, *Commun. Nonlinear Sci. Numer. Simul.*, **131** (2024), 107830. https://doi.org/10.1016/j.cnsns.2024.107830

34. V. Thomée, *Galerkin Finite Element Methods for Parabolic Problems*, $2^n d$ edition, Springer, 2006. https://doi.org/10.1007/3-540-33122-0

35. N. Liu, H. Qin, Y. Yang, Unconditionally optimal H^1-norm error estimates of a fast and linearized galerkin method for nonlinear subdiffusion equations, *Comput. Math. Appl.*, **107** (2022), 70–81. https://doi.org/10.1016/j.camwa.2021.12.012

AIMS Press